DALTON
FULL PAPER

Coordination modes of 2-mercaptonicotinic acid: synthesis and crystal structures of palladium(II), platinum(II), rhenium(III) and molybdenum(VI) complexes

Susana M. O. Quintal,[a] Helena I. S. Nogueira,*[a] Vitor Félix[a] and Michael G. B. Drew[b]

[a] *Department of Chemistry, University of Aveiro, 3810-193 Aveiro, Portugal. E-mail: helena@dq.ua.pt*
[b] *Department of Chemistry, University of Reading, Whiteknights, Reading, UK RG6 6AD*

Received 25th June 2002, Accepted 26th September 2002
First published as an Advance Article on the web 6th November 2002

New Pd(II), Pt(II), Re(III), Mo (VI) and Mo(V) complexes with 2-mercaptonicotinic acid (HnicSH), $[Pd(PPh_3)(HnicS)_2]\cdot 0.5CH_3OH$ **1**, $[Pd(HnicS)_2]\cdot CH_3OH$ **2**, $[Pt(PPh_3)(HnicS)_2]\cdot NEt_3\cdot H_2O$ **3**, $[Pt(HnicS)_2]$ **4**, $[Pt(bipy)(HnicS)_2]\cdot CH_3OH$ **5**, $[Re(PPh_3)(OCH_3)(HnicS)_2]$ **6**, $[ReI_2(PPh_3)_2(HnicS)]$ **7**, $[MoO_2(CH_3NicS)_2]$ **8** and $[Mo_2O_3(CH_3nicS)_4]\cdot DMF$ **9** have been prepared. The crystal structures of compounds **1**, **3**, **8** and $[ReI_2(PPh_3)_2(HnicS)]\cdot 0.5H_2O\cdot DMF$ (**7**·$0.5H_2O$·DMF) were determined by X-ray diffraction. Complexes **1** and **3** contain two $HnicS^-$ ligands bonded in two different coordination modes: monodentate (*S*) and chelating (*N,S*). Complexes **7** and **8** contain only one $HnicS^-$ ligand which is bidentate (*N,S*). Infrared, ^1H and ^{13}C-{^1H} NMR spectroscopic data for the complexes are presented. The Mo(VI) complex **8** is active towards oxygen atom transfer reactions and can catalyse the oxidation of benzoin and PPh_3 with dmso; the catalysis occurs *via* the Mo(V) complex **9** which has been isolated and characterized.

Introduction

Heterocyclic thiolates are ambidentate ligands that are capable of involving either the exocyclic sulfur or the endocyclic nitrogen atoms of the thioamide group in monodentate, chelating or bridging coordination.[1–3] The introduction of an acid function next to the thiol group, as in 2-mercaptonicotinic acid, leads to other coordination possibilities, such as chelating (*O,S*) and (*N,S*), presented in Scheme 1.

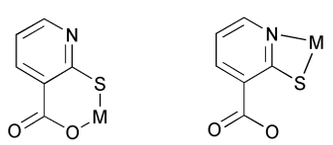

Scheme 1

Several pyridine-2-thiolate[3–15] and thiosalicylate complexes[16–19] have been reported but only a few complexes of 2-mercaptonicotinic acid (HnicSH) have been studied.[20–25] Complexes of HnicSH containing transition metals, which have been isolated include $[\{Os_3H(CO)_{10}\}_2(nicS)]$,[21] $[\{Os_3H(CO)_9\}(nicS)\{Os_3H(CO)_{10}\}]$,[21] $[M_3(HnicS)_3Cl_3]$ (M = Pd, Pt),[23] $[Ag(HnicS)]_6\cdot 4H_2O$,[24] $\{Na[Ag(nicS)]\cdot H_2O\}_n$,[24] $H[Au(HnicS)_2]$,[24] $Na_3[Au(nicS)_2]\cdot 2H_2O$,[24] $[Ag(HnicS)(PPh_3)_2]$,[25] $[Ag(HnicS)(PPh_3)_3]$[25] and $[Au(HnicS)(PPh_3)]$.[25] The crystal structures show different coordination modes to HnicSH: for the osmium complexes bridging *O,O* and *S* was found in $[\{Os_3H(CO)_{10}\}_2(nicS)]$,[21] and bridging *O,O* and *S* and monodentate *N* was found in $[\{Os_3H(CO)_9\}(nicS)\{Os_3H(CO)_{10}\}]$;[21] in the palladium complex $[Pd_3(HnicS)_3Cl_3]$[23] each ligand acts as bidentate *N,S*, with each sulfur atom bridging two palladium atoms; in the silver complex $[Ag(HnicS)]_6\cdot 4H_2O$[24] the ligand acts as bidentate *N,S* and each sulfur atom is bridging two or three silver atoms; HnicSH acts as a monodentate *S* ligand in $H[Au(HnicS)_2]$,[24] $[Ag(HnicS)(PPh_3)_2]$[24] and $[Ag(HnicS)(PPh_3)_3]$.[25] Coordination by the sulfur atom seems to be preferred in all complexes.

The coordination chemistry of heterocyclic thiols has been the subject of various studies due to its versatile bonding modes and also because similar coordination occurs in many redox active centres of metalloenzymes.[1,2,26–28] Molybdenum complexes containing the $Mo^{VI}O_2^{2+}$ group have been used as models for oxomolybdenum enzymes. These enzymes catalyse oxygen atom transfer reactions, that are usually described as involving mononuclear $Mo^{VI}O_2^{2+}$ and $Mo^{IV}O^{2+}$ species[29–35] rather than dinuclear Mo^V–O–Mo^V species. The formation of dinuclear Mo^V–O–Mo^V species is prevented by steric hindrance of the ligands, as previously reported.[31,36]

We have been interested in the coordination of aromatic ambidentate ligands such as dihydroxybenzoic acids[37] and 3-hydroxypicolinic acid[38,39] to second- and third-row transition metals. In this work, we synthesised Pd(II), Pt(II), Re(III), Mo(VI) and Mo(V) complexes with 2-mercaptonicotinic acid. The complexes were characterised by vibrational spectroscopy and NMR. The X-ray crystal structures of $[Pd(PPh_3)(HnicS)_2]\cdot 0.5CH_3OH$, $[Pt(PPh_3)(HnicS)_2]\cdot NEt_3\cdot H_2O$, $[ReI_2(PPh_3)_2(HnicS)]\cdot 0.5H_2O\cdot DMF$ and $[MoO_2(CH_3nicS)_2]$ were determined and show two different types of coordination: monodentate (*S*) and chelating (*N, S*). The oxo-transfer properties of the molybdenum complex were also studied and are consistent with the formation of a dinuclear Mo^V–O–Mo^V species.

Results and discussion

Preparations

Suspensions of *trans*-$[Pd(PPh_3)_2Cl_2]$ or *cis*-$[Pt(PPh_3)_2Cl_2]$ and HnicSH in an ethanol/methanol mixture were stirred in the presence of triethylamine to give the complexes $[Pd(PPh_3)(HnicS)_2]\cdot 0.5CH_3OH$ **1** and $[Pt(PPh_3)(HnicS)_2]\cdot NEt_3\cdot H_2O$ **3**. When $K_2[MCl_4]$ (M = Pd, Pt) was used as starting material, the compounds obtained were $[Pd(HnicS)_2]\cdot CH_3OH$ **2** and $[Pt(HnicS)_2]$ **4**. The reaction of the 2,2′-bipyridine (bipy) complexes $[M(bipy)Cl_2]$ (M = Pd, Pt) with HnicSH gave

Table 1 Bond lengths (Å) and angles (°) in the metal coordination sphere of complexes **1** and **3**

	M = Pd(II) **1**	M = Pt(II) **3**
M–N(11)	2.123(10)	2.120(8)
M–S(1)	2.326(4)	2.343(3)
M–S(2)	2.340(4)	2.322(3)
M–P(1)	2.229(3)	2.216(4)
N(11)–M–P(1)	169.5(3)	170.1(3)
P(1)–M–S(1)	99.2(1)	100.9(1)
P(1)–M–S(2)	90.5(1)	92.0(1)
N(11)–M–S(1)	70.4(3)	69.2(3)
N(11)–M–S(2)	99.7(3)	97.9(3)
S(1)–M–S(2)	169.1(1)	166.2(1)

$[Pt(bipy)(HnicS)_2]\cdot CH_3OH$ **5** with platinum, but no palladium analogue was obtained.

The complexes $[Re(PPh_3)(OCH_3)(HnicS)_2]$ **6** and $[ReI_2(PPh_3)_2(HnicS)]$ **7** were synthesised by refluxing HnicSH with $[ReO_2I(PPh_3)_2]$ in methanol and $[ReOI_2(PPh_3)_2(OCH_2CH_3)]$ in acetone, respectively. In these reactions there was formation of rhenium(III) complexes from the rhenium(V) precursors. The reduction of rhenium can be interpreted[40–42] as a result of oxygen transfer from the precursor to free PPh_3, giving $OPPh_3$ and a rhenium(III) complex. Similar results were reported[40] for the synthesis of a 4,6-dimethylpyrimidine-2-thiolate complex of rhenium, *trans*-$[Re^{III}X_2(C_6H_7N_2S)(PPh_3)_2]\cdot CH_3COCH_3$, from $[Re^{V}OX_3(PPh_3)_2]$ (X = Cl, Br). There is also a possible explanation[40] for the reduction of rhenium(V), as a result of partial oxidation of the HnicSH ligand in the thiol form, to yield the corresponding disulfide; though in this case a lower yield should have been obtained as a result of the consumption of part of the ligand.

The reaction of $[MoO_2(acac)_2]$ and HnicSH in refluxing methanol originated the esterification of the COOH group in the ligand, with formation of the complex $[MoO_2(CH_3nicS)_2]$ **8**. The reaction of **8** in DMF and in the presence of PPh_3 originated a Mo(V) complex, $[Mo_2O_3(CH_3nicS)_4]\cdot$DMF **9**.

Suitable crystals of **1**, **3**, **7**·0.5H_2O·DMF and **8** for the X-ray diffraction studies were obtained by vapour diffusion of diethyl ether into: a dichloromethane solution of complex **1**, an ethanol solution of complex **3**, a DMF solution of complex **7** and a chloroform solution of complex **8**.

Crystal structures

The crystal structures of $[Pd(PPh_3)(HnicS)_2]\cdot 0.5CH_3OH$ **1**, $[Pt(PPh_3)(HnicS)_2]\cdot NEt_3\cdot H_2O$ **3**, $[ReI_2(PPh_3)_2(HnicS)]\cdot 0.5H_2O\cdot$DMF **7**·0.5$H_2O$·DMF and $[MoO_2(CH_3nicS)_2]$ **8** were determined using single crystal X-ray diffraction.

ORTEP diagrams of the complexes **1** and **3** together with the labelling scheme adopted are shown in Fig. 1 (a) and (b), respectively. Selected bond lengths and angles are listed in Table 1, and indicate that the metal centre in both complexes is coordinated to two sulfurs, one nitrogen and one phosphorus atom in a distorted square planar coordination environment. One of the two $HnicS^-$ ligands displays a bidentate coordination fashion leading to the formation of a four membered *N,S* chelate ring with a small S–M–N bite angle of 70.4(3) and 69.2(3)° for **1** and **3**, respectively. The second $HnicS^-$ ligand is coordinated to the metal centre *via* the sulfur atom only, with a M–S distance of 2.340(4) Å in **1** and 2.322(3) Å in **3**. In both complexes the ligands adopt an identical disposition with two sulfur atoms *trans* to each other with S–M–S angles of 169.1(1)° in **1** and 166.2(1)° in **3**. The dihedral angle between the least squares plane determined by the carbon atoms of the aromatic rings is 53.1(5)° and 58.2(5)° for **1** and **3**, respectively. In addition, the molecular dimensions associated with the metal coordination sphere in these two complexes are similar suggesting that they are isostructural. In fact the match between the two structures gives a root mean square (RMS) deviation of 0.145 Å only, for 40 non-hydrogen atoms. The RMS value is reduced to 0.07 Å when the atomic coordinates of the two MPN_2S_2 fragments are considered. Protonation of the *N,S*-chelating $HnicS^-$ ligand, in complexes **1** and **3**, occurs at O(19). In both cases the hydrogen positions were tried alternatively in O(18) and O(19) and the structures shown in Fig. 1 (a) and (b) correspond to the lower *R* values. Furthermore the intermolecular interactions involving the proton bonded to O(19) have dimensions within the usual values; if the proton is bonded to O(18) it would result in senseless H ··· H short intermolecular contacts. The lengths for the metal centres are within the expected values.[43]

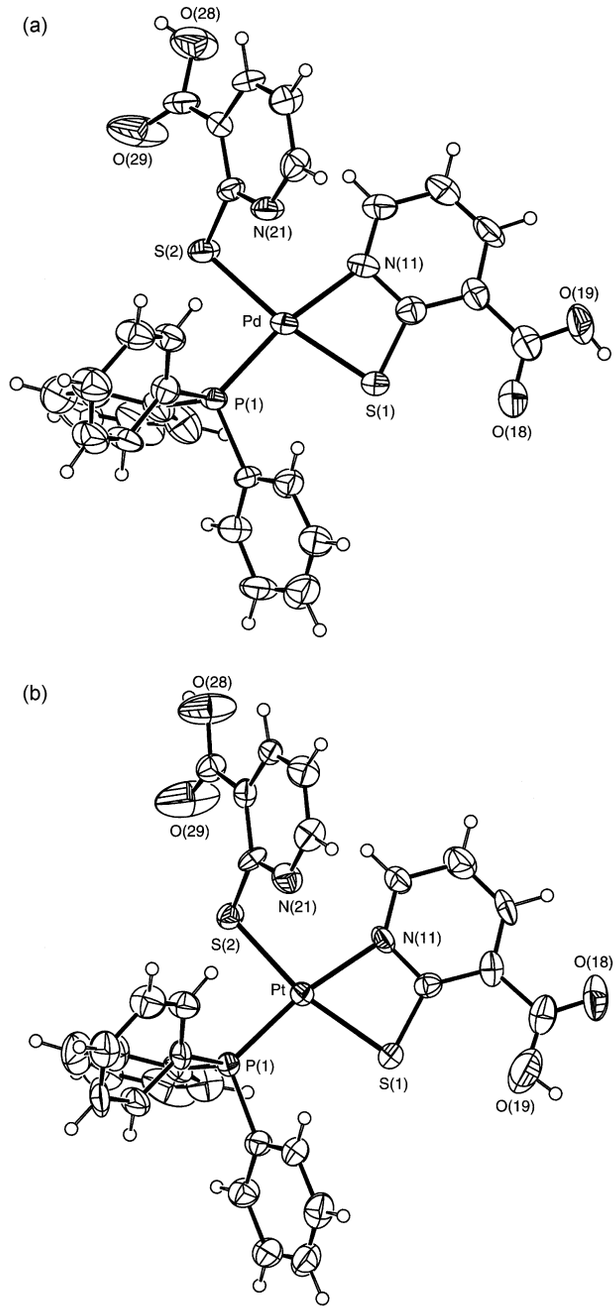

Fig. 1 ORTEP[67] views of (a) $[Pd(PPh_3)(HnicS)_2]\cdot 0.5CH_3OH$ **1** and (b) $[Pt(PPh_3)(HnicS)_2]\cdot NEt_3\cdot H_2O$ **3** showing the overall molecular geometry. Ellipsoids are drawn at 40% probability level. The labelling scheme used for the carbon atoms is omitted for clarity as are the solvent molecules.

A striking structural feature is apparent from the molecular diagrams presented in Fig. 1 (a) and (b) for complexes **1** and **3**, respectively; in both species the nitrogen atom of the $HnicS^-$

ligand, with monodentate coordination behaviour, is directed towards the metal centre leading to short intermolecular distances [Pd ··· N of 2.982(11) and Pt ··· N of 3.060(14) Å] which suggest a weak bonding interaction consistent with a [4+1] coordination type. A comparable situation was found[38] for the related complexes $[M(PPh_3)_2Cl(picOH)]$ (M = Pd(II) or Pt(II)). In both cases the 3-hydroxypicolinate ($picOH^-$) ligand is coordinated in *N*-monodentate fashion with the carboxylate group pointing to the metal centre; the distances Pd ··· O 2.773 Å and Pt ··· O 2.734(4) Å were obtained. The spatial disposition adopted by the ligands in this type of complex may reflect a delicate balance between the electronic ground states of the metal centre and the steric requirements of the ligands. The d^8 electronic configuration of Pd(II) and Pt(II) favours structures with coordination number 4, while the bulky PPh_3 ligand forces the pyridine derivative to adopt an orientation with a long M ··· N interaction, in order to minimize the steric interactions within the complex.

ORTEP diagrams of **7** and **8**, including the atomic notation scheme used, are presented in Fig. 2 and 3, respectively. Selected bond lengths and angles within the metal coordination sphere are given in Table 2. The Re(III) complex **7** contains one

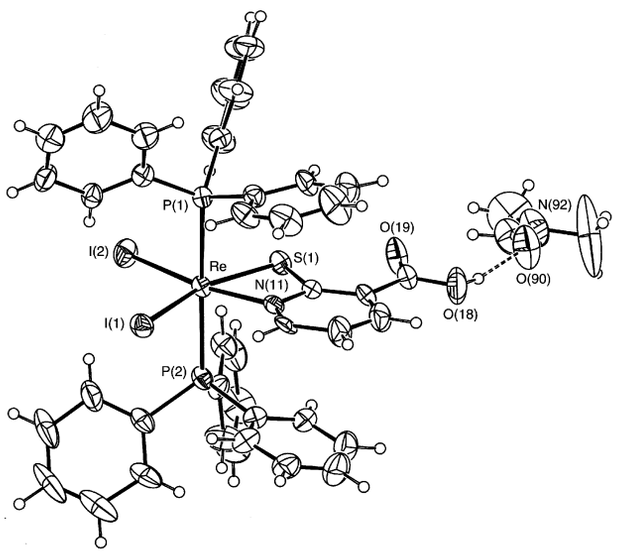

Fig. 2 An ORTEP[67] view of $[ReI_2(PPh_3)_2(HnicS)]\cdot0.5H_2O\cdot DMF$ **7**·0.5H_2O·DMF showing the overall molecular geometry. Ellipsoids are drawn at 40% probability level. The labelling scheme used for the carbon atoms is omitted for clarity.

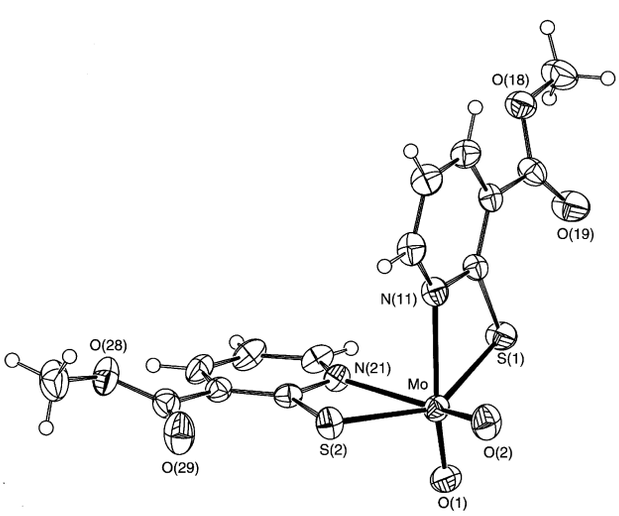

Fig. 3 An ORTEP[67] view of $[MoO_2(CH_3nicS)_2]$ **8** showing the overall molecular geometry. Ellipsoids are drawn at 40% probability level. The labelling scheme used for the carbon atoms is omitted for clarity.

Table 2 Bond lengths (Å) and angles (°) subtended at the metal centre for complexes **7**·0.5H_2O·DMF and **8**

Complex **7**			
Re–N(11)	2.111(12)	Re–S(1)	2.425(4)
Re–P(2)	2.494(5)	Re–P(1)	2.495(5)
Re–I(1)	2.711(3)	Re–I(2)	2.721(3)
N(11)–Re–S(1)	66.6(3)	N(11)–Re–P(2)	88.6(3)
S(1)–Re–P(2)	91.0(2)	N(11)–Re–P(1)	88.9(3)
S(1)–Re–P(1)	90.0(2)	P(2)–Re–P(1)	176.7(1)
N(11)–Re–I(1)	92.4(3)	S(1)–Re–I(1)	159.1(1)
P(2)–Re–I(1)	87.7(1)	P(1)–Re–I(1)	90.3(1)
N(11)–Re–I(2)	165.4(3)	S(1)–Re–I(2)	98.8(1)
P(2)–Re–I(2)	92.2(1)	P(1)–Re–I(2)	90.8(1)
I(1)–Re–I(2)	102.2(1)		
Complex **8**			
Mo–O(1)	1.697(3)	Mo–O(2)	1.701(4)
Mo–N(11)	2.309(4)	Mo–N(21)	2.317(5)
Mo–S(2)	2.445(2)	Mo–S(1)	2.452(2)
O(1)–Mo–O(2)	106.8(2)	O1–Mo–N(11)	154.6(1)
O(2)–Mo–N(11)	90.2(2)	O(1)–Mo–N(21)	90.2(2)
O(2)–Mo–N(21)	155.4(2)	N(11)–Mo–N(21)	80.5(2)
O(1)–Mo–S(2)	107.4(1)	O(2)–Mo–S(2)	92.7(2)
N(11)–Mo–S(2)	90.0(1)	N(21)–Mo–S(2)	64.8(1)
O(1) –Mo–S(1)	91.7(1)	O(2)–Mo–S(1)	108.4(1)
N(11)–Mo–S(1)	64.6(1)	N(21)–Mo–S(1)	88.3(1)
S(2)–Mo–S(1)	146.3(1)		

$HnicS^-$ unit while the Mo(VI) complex **8** presents two methyl ester derivatives of the HnicSH acid. The complexes are six-coordinated and both $HnicS^-$ and its derivative CH_3nicS^- ligands exhibit again the *N,S* coordination mode rather than *O,S* coordination.

In complex **7** the Re(III) centre shows a distorted octahedral coordination with the equatorial plane determined by two iodine atoms, one sulfur and one nitrogen atom both from the $HnicS^-$ ligand. The axial positions are occupied by two phosphorus atoms from the PPh_3 ligands. The $HnicS^-$ ligand is approximately perpendicular to the PReP vector leading to an angle between this vector and the plane defined by the carbon atoms of the aromatic ring of 89.4(4)° and a sandwich containing the $HnicS^-$ ligand between two PPh_3 ligands is formed. This geometric arrangement may be determined by minimisation of the steric interactions between the bulky PPh_3 ligands and the $HnicS^-$ ligand. A slightly differential *trans* effect is apparent from the values of the Re–N, Re–S and Re–I distances. The Re–I(1) bond [2.711(3) Å] *trans* to the Re–S(1) bond [2.425(4) Å] is 0.01 Å shorter than the Re–I(2) bond [2.721(3) Å] *trans* to the Re–N(11) bond [2.111(12) Å]. These distances are comparable to those reported in the literature for Re(III) complexes containing a I_2SN donor set.[43]

In complex **8** the coordination environment of the Mo(VI) centre can be described as a distorted octahedron. The two CH_3nicS^- ligands are in different coordination planes: one is axial and the other is equatorial; consequently the aromatic rings are almost perpendicular making an angle of 89.5(1)°, which is near the ideal value of 90°. On the other hand, the bond angles between *trans* donor atoms N–Mo=O and S–Mo–S display a significant deviation of *ca.* 30° from 180°. The steric demands of the N–Mo-S bite angle of the CH_3nicS^- ligand precludes the sulfur and nitrogen donor atoms from achieving the ideal positions of an octahedron. Indeed all four complexes reported here present acute N–M–S chelating angles. Thus in **8** the two N–Mo-S angles are 64.6(1) and 64.8(1)° while in **7** a slightly larger value for the N–Re–S chelating angle of 66.6(3)° was found.

The crystal structure of **1** is built up from an asymmetric unit composed of one $[Pd(PPh_3)(HnicS)_2]$ discrete molecule and one CH_3OH solvent molecule, while the crystal structure of **3** is made up from one $[Pt(PPh_3)(HnicS)_2]$ molecule and two solvate

Table 3 Analytical and spectroscopic data for complexes of 2-mercaptonicotinic acid and the free ligand

Compound	Analysis[a](%)				Vibrational spectra[b]/cm^{-1}					
	C	H	N	S	ν(C=O)	ν(C=N)	ν(C–O)	ν(C=S)	ν(M–N)	ν(M–S)
2-Mercaptonicotinic acid					1679 vs	1597 s	1332 s	1142 m		
					1680(3)	*1580(4)*	*1332(1)*	*1140(3)*		
$[Pd(PPh_3)(HnicS)_2]\cdot 0.5CH_3OH$ **1**	53.6	3.5	4.1	9.0	1706 s	1590 vs	1377 vs	1127 s	371 m	317 vw
	(52.9)	(3.6)	(4.0)	(9.3)	*1710(1)*	*1586(5)*	*1377(2)*	*1131(3)*	*356(3)*	*312(1)*
$[Pd(HnicS)_2]\cdot CH_3OH$ **2**	34.8	2.3	6.5	14.6	1677 vs	1563 vs	1398 vs	1132 vs	384 m	345 m
	(34.9)	(2.7)	(6.3)	(14.3)	*1714(1)*	*1572(4)*	*1399(1)*	*1133(4)*	*385(1)*	*344(1)*
$[Pt(PPh_3)(HnicS)_2]\cdot NEt_3\cdot H_2O$ **3**	49.1	5.1	4.7	6.6	1700 s	1595 vs	1377 vs	1129 s	387 w	–
	(48.9)	(4.6)	(4.7)	(7.2)	*1710(1)*	*1588(5)*	*1379(2)*	*1132(3)*	*360(1)*	*306(1)*
$[Pt(HnicS)_2]$ **4**	27.1	2.1	5.7	13.1	1677 vs	1567 vs	1400 vs	1132 vs	392 w	354 w
	(28.6)	(1.6)	(5.6)	(12.7)	*1714(1)*	*1572(5)*	*1400(1)*	*1132(4)*	*395(1)*	*352(1)*
$[Pt(bipy)(HnicS)_2]\cdot CH_3OH$ **5**	35.7	3.2	7.9	9.2	1713 vs	1580 vs	1380 s	1134 s	387 w	350 w
	(39.9)	(2.9)	(8.1)	(9.3)	*1709(1)*	*1571(5)*	*1399(1)*	*1133(4)*	*375(1)*	*344(1)*
$[Re(PPh_3)(OCH_3)(HnicS)_2]$ **6**	46.2	3.5	3.2	8.7	1717 vs	1570 vs	1398 vs	1132 vs	447 w	425 w
	(47.3)	(3.3)	(3.6)	(8.1)						
$[ReI_2(PPh_3)_2(HnicS)]$ **7**	45.5	3.7	1.2	2.7	1706 vs	1563 s	1384 s	1129 vs	449 w	416 w
	(45.1)	(3.1)	(1.3)	(2.9)	–	*1572(2)*	*1396(1)*	*1133(1)*	*501(1)*	*425(1)*
$[MoO_2(CH_3nicS)_2]$ **8**	35.2	3.1	6.2	14.9	1725 vs	1567 vs	1402 vs	1131 s	372 s	352 s
	(36.2)	(2.6)	(6.0)	(13.8)	*1720(3)*	*1570(4)*	*1404(1)*	*1139(3)*	*365(3)*	*345(1)*
$[Mo_2O_3(CH_3nicS)_4]\cdot DMF$ **9**	36.4	3.9	6.8	13.3	1725 vs	1568 s	1400 vs	1134 s	374 w	342 w
	(37.8)	(3.2)	(7.1)	(13.0)	*1724(3)*	*1569(9)*	*1400(1)*	*1135(1)*	–	*326(6)*

[a] Calculated values in parentheses. [b] Raman data in italics.

molecules, one of NEt_3 and one of H_2O. In spite of the different contents of the unit cells of these two compounds they crystallize in the same chiral space group $P2_1$. Furthermore, self-assembly of $[M(PPh_3)(HnicS)_2]$ results in both cases in the formation of a 1-D polymeric structure anchored by hydrogen bonding interactions between the free carboxylic groups of two neighbouring molecules, as illustrated in Fig. 4 for the Pd

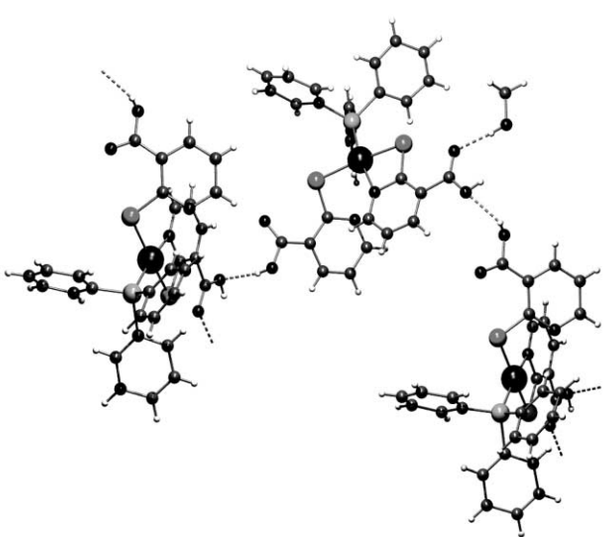

Fig. 4 Hydrogen bonded 1-D polymer of $[Pd(PPh_3)(HnicS)_2]\cdot 0.5CH_3OH$ **1**, viewed along the *z* axis.

complex. The dimensions of the OH ··· O(H)C hydrogen bonds in **1** are H(28) ··· O(19) [1 − *x*, 1/2 + *y*, 1 − *z*] 2.06 Å, O(28)–H(28) ··· O(19) 120.9°, O(28) ··· O(19) 2.58(2). The dimensions of the OH ··· O=C hydrogen bonds in **3** are H(28) ··· O(18) [1 − *x*, 1/2 + *y*, −*z*] 1.76 Å, O(28)–H(28) ··· O(18) 164.3°, O(28) ··· O(18) 2.55(2) Å. In addition, in **1** some of the carboxylic groups of the *N,S* coordinated $HnicS^-$ ligand, interact with CH_3OH molecules *via* one C=O ··· H–O hydrogen bond [O(18) ··· H(91) 1.90 Å, O(18) ··· H(91)–O(91) 172.5°, O(18) ··· O(91) 2.71(3) Å]. A comparable situation happens with the supramolecular structure of **3**, in which the complex molecules interact with mother liquor waters through CO–H ··· O hydrogen bonds as suggested by the short O(W1) ··· O(19) distance of 2.49 Å [H(19) ··· O(W1) 2.16 Å, O(19)–H(19) ··· O(W1) 104.1°] and with triethylamine molecules thorough C–H ··· O(H)C hydrogen bonds [H(81B) ··· O(19) [−*x*, 1/2 + *y*, −*z*] 2.56 Å, C(81)–H(81B) ··· O(19) 137.4°, C(81) ··· O(19) 3.34(3) Å].

In the crystal structure of $\mathbf{7}\cdot 0.5H_2O\cdot DMF$ the molecules of $[ReI_2(PPh_3)_2(HnicS)]$ and DMF are connected *via* a hydrogen bonding interaction with the following dimensions: H(18) ··· O(90) 1.83 Å, O(18)–H(18) ··· O(90) 166.4°, O(18) ··· O(90) 2.63(2) Å. The analysis of intermolecular interactions for complex **8** did not show any relevant structural features.

Vibrational spectra

Infrared and Raman spectroscopic data for HnicSH and its complexes are shown in Table 3; tentative assignments are based on those found in the literature for HnicSH,[23,24,44] heterocyclic thiones[45–47] and thiosalicylic acid complexes.[16,19]

2-Mercaptonicotinic acid shows the characteristic thione–thiol tautomerism[1] (Scheme 2). The absence, in the infrared

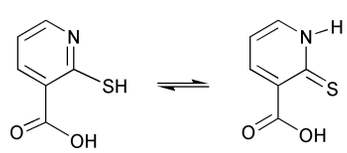

Scheme 2

spectrum of the free HnicSH ligand, of a ν(S–H) absorption band at *ca.* 2500 cm^{-1},[16,47] and the presence of the ν(N–H) absorption[46–48] at 3186 cm^{-1} and ν(C=S) at 1142 cm^{-1}, suggest that the ligand in the solid state exists in the thione rather than the thiol form. This is in agreement with what was found for similar ligands, such as pyrimidine-2-thione,[45] 2-mercaptobenzothiazole,[47] 2-mercaptopyridine[13,49,50] and its derivatives.[51]

The position of the bands assigned to the ν(C=O) carboxyl stretch, in the vibrational spectra of complexes **1** to **9** (with the exception of **2** and **4**), at wavenumbers over 1700 cm^{-1}, clearly indicates[37–39,52] that in these compounds the carboxyl group is protonated (or esterification has occurred, as in the case of compounds **8** and **9**) and it is not coordinated to the metal centres, as shown in the crystal structures of **1**, **3** and **7**. The infrared and Raman spectra of the free HnicSH ligand show

Table 4 ^{1}H and ^{13}C-{^{1}H} NMR spectroscopic data for 2-mercaptonicotinic acid and its complexes[a]

Compound	H_4	H_5	H_6	C_2	C_3	C_4	C_5	C_6	C_7	C_{ester}
2-Mercaptonicotinic acid[b]	8.15	7.12	8.51	165.3	129.6	143.3	115.1	143.9	173.2	
				168.5	*124.7*	*144.9*	*117.2*	*147.9*	*171.7*	
$[Pd(PPh_3)(HnicS)_2]\cdot 0.5CH_3OH$ **1**	7.96	6.76	8.13	148.1	129.4	139.7	116.6	129.6	168.7	
				149.8	*130.8*	*141.6*	*118.9*	*135.8*	*169.5*	
				142.8	*129.2*	*140.8*	*113.4*	*133.9*	*167.6*	
$[Pd(HnicS)_2]\cdot CH_3OH$ **2**[b]	8.20	7.07	8.55	*152.9*	*124.0*	*139.6*	*117.2*	*144.7*	*170.4*	
	7.95	6.94	8.23							
$[Pt(PPh_3)(HnicS)_2]\cdot NEt_3\cdot H_2O$ **3**	8.17	6.87	8.17	148	129.1	139.0	116.9	130.0	169.4	
				149.9	*130.7*	*141.9*	*119.1*	*135.6*	*169.1*	
				141.9	[e]	*140.7*	*113.5*	[e]	*168.0*	
$[Pt(HnicS)_2]$ **4**[b]	8.28	7.22	8.72	*153.0*	*125.2*	*138.3*	*118.0*	*138.3*	*170.2*	
	8.27	7.11	8.33							
	8.09[f]	6.98[f]	8.19[f]							
$[Pt(bipy)(HnicS)_2]\cdot CH_3OH$ **5**[c]	7.87	7.23	9.09							
	7.65	7.16	8.81							
$[ReI_2(PPh_3)_2(HnicS)]$ **7**[b]	11.53	7.61	11.88	*143.3*	*127.6*	*134.8*	*115.5*	*132.6*	*173.2*	
$[MoO_2(CH_3nicS)_2]$ **8**	8.34	7.11	8.71	164.0	125.1	142.4	119.3	148.1	170.0	52.7
				164.4	*124.0*	*146.7*	*121.4*	*150.2*	*169.2*	*53.7*
				163.6	*125.9*	*140.4*	*120.9*	*148.3*		*53.0*
$[Mo_2O_3(CH_3nicS)_4]\cdot DMF$ **9**[d]	8.30	7.01	8.68	154.8	116.5	139.2	108.3	132.9	168.2	[e]
	8.01	6.78	8.50	154.1	115.1	138.2	107.0	131.0	160.8	[e]

[a] Spectra in $CDCl_3$ solution unless otherwise stated; CPMAS solid state NMR data in italics. [b] In $(CD_3)_2SO$. [c] In CD_3OD. [d] In CD_2Cl_2 [e] Peak obscured. [f] New species in solution.

ν(C=O) at a low wavenumber (1679 cm^{-1}), when compared to the spectra of the complexes; this is possibly due to hydrogen bonding in HnicSH, also shown by the presence of several bands in the 3012–2812 cm^{-1} region. A similar explanation can be given for the values of ν(C=O) in complexes **2** and **4** (1677 cm^{-1}), very similar to that in the free ligand.

In the free ligand IR and Raman spectra, the band at 1597 cm^{-1} is mainly assigned to the ν(C=N) vibration.[51] In general, the spectra of the complexes exhibit the ν(C=N) stretching mode shifted to lower wavenumber, with an increase in intensity. The band assigned to ν(C=S)[48] at 1142 cm^{-1} shifts to lower wavenumber on coordination.

In the infrared and Raman spectra of the Mo(VI) complex **8**, the symmetric *cis*-dioxo stretch, $\nu_{sym}(MoO_2)$, is seen as a very strong band at 932 cm^{-1}, and the asymmetric stretch, $\nu_{asym}(MoO_2)$, corresponds to a strong band at 903 cm^{-1}, weaker in the Raman. For the Mo(V) complex **9**, both infrared and Raman spectra show a very strong band at 950 cm^{-1} assigned to the ν(MoO) stretch of the Mo=O terminal group; another band at 762 cm^{-1} can possibly be assigned to the $\nu(Mo_2O)$ stretch of the bridging Mo–O–Mo group.[39] In addition to the above, PPh_3 and bipy bands were observed in all the applicable spectra.

The proposed formula for complexes **2**, **4** to **6** and **9** are based on elemental analysis and spectroscopic data, considering analogous complexes that have been reported for chelating *N,S* and other bidentade ligands.[6,38,45,53]

^{1}H and ^{13}C-{^{1}H} NMR spectra

Proton and carbon NMR data and tentative assignments for HnicSH (see Chart 1 for labelling) and the complexes are given in Table 4. Tentative assignments are based on those found in the literature for HnicSH[24,25] and similar heterocyclic thionate complexes.[48,51,54]

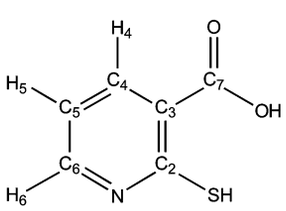

Chart 1

The ^{1}H NMR spectra of HnicSH in dmso-d_6, shows a triplet at 7.12 ppm assigned to the H_5 proton, a double-doublet at 8.15 ppm assigned to H_4 and another double-doublet at 8.51 ppm assigned to H_6. The absence of any evidence for the thiol proton (SH, δ = 2–5 ppm)[45] confirms the thione form as the dominant species of HnicSH in dmso-d_6 solution, as in the solid state (shown by the infrared and Raman spectra). Also, a broad signal at about 14.6 ppm may be assigned[51] to the NH proton; it is absent in the spectra of the complexes. In general, the resonances of the ring protons of the coordinated $HnicS^-$ ligand, show small upfield shifts in the ^{1}H NMR spectra of the complexes, with the exception of complex **7**. In complex **7** the resonances of the ring protons of the ligand shift downfield, possibly as a result of the unpaired electrons in the rhenium(III) centre. In contrast with complexes **1** and **3**, a large downfield shift is also observed for the protons of the PPh_3 phenyl rings in **7** (two broad signals at 14.1 and 8.9 ppm with an intensity ratio of 2 : 3, were assigned to the *ortho*, 12H, and *para* and *meta* protons, 18H). In the $[MoO_2(CH_3nicS)_2]$ **8** ^{1}H NMR spectra the signal of the methyl ester group is observed at 3.98 ppm; and in the case of $[Mo_2O_3(CH_3nicS)_4]\cdot DMF$ **9** at 3.93 ppm. The ^{1}H NMR spectra in dmso-d_6 of complexes **2** and **4** show two different sets of peaks corresponding to the two ligand molecules in each compound; a third set of peaks in the case of **4**, with different intensity, indicates the formation of another species in solution. However, for **2** and **4** only one set of peaks could be clearly identified in the solid state ^{13}C NMR spectra.

In the ^{13}C NMR spectra of the complexes, the C–S carbon of the $HnicS^-$ ligand, C_2, shows a downfield shift of over 10 ppm (only less than this in the case of the molybdenum complex **8**). This C_2 shift supports coordination through the sulfur atom. There is also a considerable downfield shift in C_6, shown in the spectra of the complexes. The significant shifts in the resonances of C_2 and C_6 together with the fact that the position of the carboxylic carbon atom C_7 is little altered, is consistent with *N,S*-chelation in the complexes (shown in the crystal structures of **1**, **3**, **7** and **8**).

The ^{13}C NMR spectra in $CDCl_3$ of complexes **1** and **3** show similar chemical shifts, the signals are broad which implies that in solution, there might be a rapid inter-conversion between the two $HnicS^-$ ligands (monodentade (*S*) and bidentade (*N,S*)), possibly *via* a five-coordinate intermediate.[6] In the solid state ^{13}C NMR spectra of both **1** and **3**, two different sets of peaks are observed corresponding to the two ligands.

Oxo-transfer properties of the molybdenum complexes

The oxo-transfer properties of $[MoO_2(CH_3nicS)_2]$ **8** were studied using benzoin (1,2-diphenyl-2-hydroxyethanone) and PPh_3 (triphenylphosphine) as substrates.[30,31,55,56]

The catalytic properties of **8** for benzoin oxidation were investigated using dimethyl sulfoxide (dmso) as the oxo donor. The complex was able to catalyse the oxidation of benzoin to benzil (1,2-diphenylethane-1,2-dione) by dmso. The reaction was monitored by ^1H NMR spectroscopy, which allowed the quantification of benzoin and benzil. The percentage conversion of benzoin to benzil was 75% after 6 hours, and about 100% after 24 hours. Similar results were previously reported[39] for the polynuclear molybdenum complexes $(^nBu_4N)_2[Mo_4O_{12}(picOH)_2]$ and $(^nHex_4N)_2[Mo_2O_6(picOH)_2]$ (HpicOH = 3-hydroxypicolinic acid).

Complex **8** was tested as catalyst for PPh_3 oxidation using again dmso as the oxo donor. The oxidation of PPh_3 using molybdenum(VI) complexes is usually monitored using UV-visible absorption,[30,31,57] by the intensity decrease in the Mo(VI) band and the intensity increase in a new Mo(V) or Mo(IV) band. In the reaction with complex **8**, we did not observe a Mo(V) or Mo(IV) band over a reaction period of 3 hours. The reaction was then monitored by ^{31}P NMR spectroscopy (Fig. 5: PPh_3, −5.6 ppm; $POPh_3$, 26.7 ppm). The reaction of **8** and 20 equivalents of PPh_3 was performed in dmso-d_6, at room temperature. The complex shows catalytic activity and the percentage conversion of PPh_3 to $POPh_3$ was 42% after 6 hours, and 90% after 24 hours. To observe the visible spectrum of the reduced form of complex **8**, a similar reaction was performed in dichloromethane, in the absence of dmso. The reaction was monitored using the visible spectra and in fact, the intensity of the band at 371 nm characteristic of the Mo(VI) complex **8** (Fig. 6a) strongly decreased during reaction and new bands at 504 and 540 nm appeared with increasing intensity, corresponding to a Mo(V) compound. The final spectrum is similar to that of the Mo(V) species isolated and characterised as $[Mo_2O_3(CH_3nicS)_4]$ **9** (Fig. 6b).

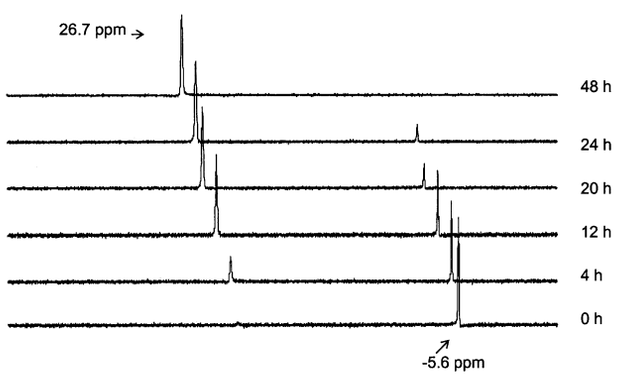

Fig. 5 Evolution of PPh_3 oxidation to $POPh_3$ in dmso-d_6, using $[MoO_2(CH_3nicS)_2]$ **8** as catalyst, as monitored by ^{31}P NMR.

The catalytic cycle proposed is shown in Scheme 3. If step b is fast, the reduced form of the catalyst is rapidly converted to its oxidised form, complex **8**; which can explain the absence of the Mo(V) band in the UV-visible spectra, during the catalytic reaction in dmso. These results are consistent with other oxygen atom transfer reactions involving active dinuclear Mo^V–O–Mo^V species.[35,53,57,58] Moreover, following a 1 : 1 addition of $[MoO_2(CH_3nicS)_2]$ **8** and PPh_3 in a CD_2Cl_2 solution, the ^{31}P NMR spectra show that after 4 hours a 50% conversion of PPh_3 to $POPh_3$ was achieved without further reaction, which corresponds to the complete consumption of **8** according to the reaction:

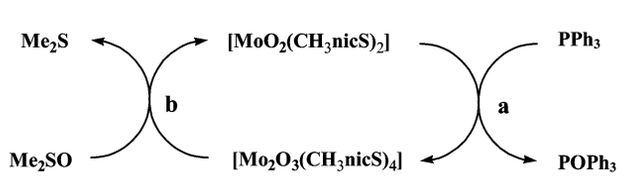

Scheme 3

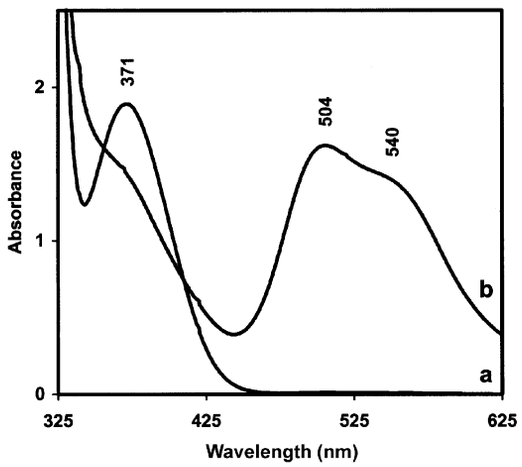

Fig. 6 UV-Visible spectra of the molybdenum complexes (a) $[MoO_2(CH_3nicS)_2]$ **8** and (b) $[Mo_2O_3(CH_3nicS)_4]\cdot DMF$ **9**, in CH_2Cl_2 solution.

$$2[MoO_2(CH_3nicS)_2] + PPh_3 \longrightarrow [Mo_2O_3(CH_3nicS)_4] + POPh_3$$

The proton NMR of the final solution presents the characteristic signals of complex $[Mo_2O_3(CH_3nicS)_4]$ **9**, which strongly suggests that this is the intermediate Mo(V) compound in the catalytic cycle as shown in Scheme 3.

Assuming that the regeneration of the Mo(VI) complex (step b in Scheme 3) is fast, its concentration should be essentially constant throughout the reaction. The rate of oxidation of the substract (benzoin or PPh_3), k_1 (step a in Scheme 3), can thus be described as corresponding to a pseudo-first order reaction: $-d[S]/dt = k_{obs}[S]$, where $k_{obs} = k_1[catalyst]$ and S = benzoin or PPh_3. Fig. 7 shows the variation of $\ln([PPh_3]_0/[PPh_3])$ *versus* time, where $[PPh_3]_0$ is the initial concentration of PPh_3. The values of the k_{obs} are 0.0038 s^{-1} (k_1 = 19.0 × 10^{-2} M^{-1} s^{-1}) for benzoin and 0.0017 s^{-1} (k_1 = 14.2 × 10^{-2} M^{-1} s^{-1}) for PPh_3. These results are based on the first 6 and 24 hours for the oxidation of benzoin and PPh_3, respectively.

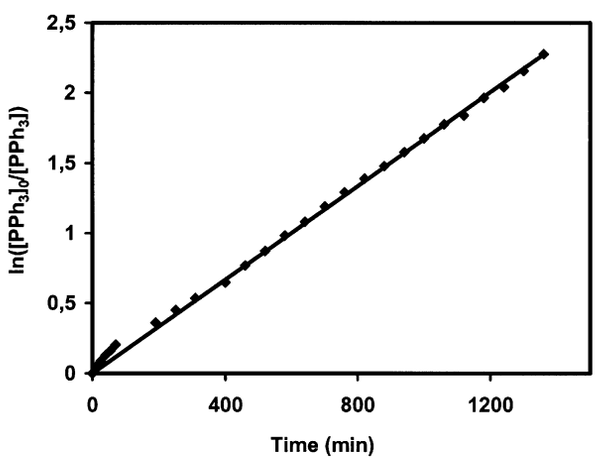

Fig. 7 Plot of $\ln([PPh_3]_0/[PPh_3])$ *versus* time using $[MoO_2(CH_3nicS)_2]$ **8** as catalyst.

Experimental

Preparation of complexes

All chemicals were of at least reagent grade and used as supplied by Aldrich. The starting complexes, *trans*-$[Pd(PPh_3)_2Cl_2]$,[59] *cis*-$[Pt(PPh_3)_2Cl_2]$,[60] $[Pt(bipy)Cl_2]$,[61] $[ReO_2I(PPh_3)_2]$,[62] $[ReOI_2(PPh_3)_2(OCH_2CH_3)]$[62] and $[MoO_2(acac)_2]$[63] were prepared by the respective literature procedures.

$[Pd(PPh_3)(HnicS)_2]\cdot 0.5CH_3OH$ (1). To a stirred suspension of *trans*-$[Pd(PPh_3)_2Cl_2]$ (0.35 g, 0.5 mmol) in ethanol (10 cm^3) was added a methanolic suspension (4 cm^3) of 2-mercaptonicotinic acid (0.16 g, 1 mmol) and triethylamine (0.28 cm^3, 2 mmol) giving an orange solution. Addition of diethyl ether resulted in the formation of orange crystals. The crystals were filtered off, washed with diethyl ether and dried over silica gel. Yield: 0.32 g, 0.46 mmol, 92%. Orange X-ray quality crystals of **1** were obtained by vapour diffusion of diethyl ether into a solution of the compound in CH_2Cl_2.

$[Pd(HnicS)_2]\cdot CH_3OH$ (2). To a stirred suspension of HnicSH (0.16 g, 1 mmol) in methanol (4 cm^3) was added an aqueous solution (5 cm^3) of $K_2[PdCl_4]$ (0.14 g, 0.5 mmol). The resulting orange suspension was stirred for one day. It was centrifuged and an orange solid isolated, washed with ethanol and acetonitrile and dried over silica gel. Yield: 0.16 g, 0.36 mmol, 72%.

$[Pt(PPh_3)(HnicS)_2)]\cdot NEt_3\cdot H_2O$ (3). To a stirred suspension of *cis*-$[Pt(PPh_3)_2Cl_2]$ (0.20 g, 0.25 mmol) in ethanol (5 cm^3) was added a methanolic suspension (2 cm^3) of HnicSH (0.08 g, 0.5 mmol) and triethylamine (0.14 cm^3, 1 mmol), resulting in a yellow solution. Addition of diethyl ether originated formation of yellow crystals. The crystals were filtered off, washed with diethyl ether and dried over silica gel. Yield: 0.16 g, 0.18 mmol, 72%. Yellow crystals of **3** suitable for X-ray diffraction were obtained by vapour diffusion of diethyl ether into a solution of the compound in ethanol.

$[Pt(HnicS)_2]$ (4). A supension of HnicSH (0.06 g, 0.4 mmol) and $K_2[PtCl_4]$ (0.08 g, 0.2 mmol) in methanol (10 cm^3) was stirred for three days. The resulting yellow suspension was centrifuged and a yellow solid isolated, washed with ethanol and dried over silica gel. Yield: 0.10 g, 0.19 mmol, 96%.

$[Pt(bipy)(HnicS)_2]\cdot CH_3OH$ (5). To a stirred suspension of $[Pt(bipy)Cl_2]$ (0.06 g, 0.15 mmol) in ethanol (5 cm^3) was added a methanolic suspension (3 cm^3) of HnicSH (0.05 g, 0.3 mmol). The resulting orange suspension was stirred for one day. It was centrifuged and an orange solid isolated, washed with ethanol and dried over silica gel. Yield: 0.09 g, 0.13 mmol, 87%.

$[Re(PPh_3)(OCH_3)(HnicS)_2]$ (6). A brownish suspension of $[ReO_2I(PPh_3)_2]$ (0.17 g, 0.2 mmol) and HnicSH (0.06 g, 0.4 mmol) in methanol (20 cm^3) was refluxed for 5 hours. To the dark red solution obtained was added 40 cm^3 of water and a dark suspension was obtained. It was centrifuged and a dark red solid isolated, washed with water and dried over silica gel. Yield: 0.11 g, 0.14 mmol, 70%.

$[ReI_2(PPh_3)_2(HnicS)]$ (7). A suspension of $[ReOI_2(PPh_3)_2(EtO)]$ (0.31 g, 0.3 mmol) and HnicSH (0.05 g, 0.3 mmol) in acetone (7 cm^3) was refluxed under N_2 for two hours. The resulting dark suspension was centrifuged and a dark red solid isolated, washed with acetone and dried over silica gel. Yield: 0.16 g, 0.14 mmol, 48%. Dark red crystals suitable for X-ray diffraction were obtained by vapour diffusion of diethyl ether into a solution of compound **7** in DMF, giving the crystalline compound $[ReI_2(PPh_3)_2(HnicS)]\cdot 0.5H_2O\cdot DMF$.

$[MoO_2(CH_3nicS)_2]$ (8). To a methanolic solution (50 cm^3) of $[MoO_2(acac)_2]$ (0.33 g, 1 mmol) was added a methanolic solution (130 cm^3) of HnicSH (0.16 g, 1 mmol) under N_2. The resulting solution was refluxed for 30 hours. After evaporation of part of the solvent a brownish solid was isolated, washed with a small volume of methanol and dried over silica gel. Yield: 0.16 g, 0.34 mmol, 68%. Brownish crystals of **8** suitable for X-ray diffraction were obtained by vapour diffusion of diethyl ether into a solution of the compound in chloroform.

$[Mo_2O_3(CH_3nicS)_4]\cdot DMF$ (9). To a DMF solution (2.5 cm^3) of $[MoO_2(CH_3nicS)_2]$ **8** (0.037g, 0.08 mmol) was added a DMF solution (2.5 cm^3) of PPh_3 (0.031 g, 0.22 mmol), under N_2. The resulting pink solution was stirred at room temperature for 5 hours. Diethyl ether was added and after 2 weeks in the fridge, a pink solid was filtered off, washed with diethyl ether and dried over silica gel. Yield: 0.013 g, 0.013 mmol, 33%.

Oxo-transfer reactions

The benzoin oxidation reaction was carried out using the method of Wong *et al.*[56] Complex **8** (0.01 mmol) and 25 equivalents of benzoin were dissolved in deoxygenated CD_3SOCD_3 (0.5 cm^3). The mixture was sealed in NMR tubes under nitrogen and heated at 100 °C. The reaction was monitored by ^1H NMR spectroscopy.

For PPh_3 oxidations, complex **8** and 20 equivalents of PPh_3 were added to CD_3SOCD_3, at room temperature. The reaction was monitored by ^{31}P NMR spectroscopy.

Crystallography

A summary of the crystallographic data together with data collection and the refinement details for $[Pd(PPh_3)(HnicS)_2]\cdot 0.5CH_3OH$ **1**, $[Pt(PPh_3)(HnicS)_2]\cdot NEt_3\cdot H_2O$ **3**, $[ReI_2(PPh_3)(HnicS)]\cdot 0.5H_2O\cdot DMF$ **7**$\cdot 0.5H_2O\cdot DMF$ and $[MoO_2(CH_3nicS)_2]$ **8** are given in Table 5. X-Ray data sets for these four complexes were collected on a MAR research image plate system equipped with graphite-monochromated Mo-Kα radiation (0.71073 Å). 95 Frames were measured at 2° intervals using a counting time adequate to the crystal under study. Data analysis was performed with the XDS program.[64] Intensities for complexes **3** and **7** were corrected empirically for absorption effects with the DIFABS program,[65] using a version modified for the image plate system, while no absorption correction was applied to complexes **1** and **8**. The structures were solved by direct methods and refined by full-matrix least-squares methods against F^2 using SHELXS and SHELXL from the SHELX97 package.[66] The occupation factors of the solvent molecules CH_3OH in **1** and H_2O in **3** were set to 0.5 in agreement with their electronic densities in the corresponding Fourier maps. All non-hydrogen atoms were refined using anisotropic thermal parameters, except the oxygen atom of the H_2O molecule in **3**, which was refined with an isotropic temperature factor. The hydrogen atoms were inserted in idealised positions and allowed to refine, riding on the parent C(O) atom with an isotropic thermal parameter equal to 1.2 times those to which they were bonded. The hydrogen atoms of the H_2O molecule were not included in the refinement.

Molecular and crystal packing diagrams were drawn with PLATON graphical software.[67]

CCDC reference numbers 188470–188473.

See http://www.rsc.org/suppdata/dt/b2/b206101e/ for crystallographic data in CIF or other electronic format.

Instrumentation

Infrared spectra were measured as KBr pellets on a Mattson 7000 FT instrument. Raman spectra were recorded on a Brüker RFS100/S FT instrument (Nd:YAG laser, 1064 nm excitation). ^1H and ^{13}C NMR spectra were recorded on a Brüker AMX300

Table 5 Room temperature crystal data and the pertinent refinement parameters for metal complexes **1**, **3**, **7**·0.5H_2O·DMF and **8**

Compound	**1**	**3**	**7**·0.5H_2O·DMF	**8**
Empirical formula	$C_{30.5}H_{25}N_2O_{4.50}PPdS_2$	$C_{36}H_{39}N_3O_5PPtS_2$	$C_{45}H_{42.50}I_2N_2O_{3\cdot50}P_2ReS$	$C_{14}H_{12}MoN_2O_6S_2$
M	693.02	884.89	1201.31	464.32
Crystal system	Monoclinic	Monoclinic	Monoclinic	Orthorhombic
Space group	$P2_1$	$P2_1$	$P2_1/c$	*Pbca*
a/Å	10.177(14)	10.390(15)	11.068(16)	8.128(14)
b/Å	17.733(27)	17.781(20)	23.569(26)	28.616(35)
c/Å	11.431(16)	11.553(15)	18.371(24)	14.941(17)
β/°	115.72(1)	115.54(1)	96.26(1)	(90.0)
V/Å^3	1859(5)	1926(4)	4764(11)	3475(8)
Z	2	2	4	8
D_c/g cm^{-3}	1.238	1.526	1.675	1.775
μ/mm^{-1}	0.687	3.836	3.998	1.028
F(000)	702	884	2326	1856
Reflections measured	3962	6141	8431	11034
Unique reflections	3962	6141	8431 (R_{int} = 0.0643)	3113 (R_{int} = 0.0226)
Final *R* indices				
R_1 and wR_2[a] [$I > 2\sigma(I)$]	0.0679, 0.1850	0.0449, 0.1176	0.0973, 0.1750	0.0441, 0.0843
R_1 and wR[a] (all unique data)	0.0923, 0.2045	0.0546, 0.1241	0.1259, 0.1860	0.0584, 0.0909

[a] $R_1 = \Sigma(\Delta F)/\Sigma(F_o)$, $wR_2 = \{\Sigma[w\Delta(F^2)^2]/\Sigma[w(F_o^2)^2]\}^{\frac{1}{2}}$, $w = 1/[\sigma^2(F_o^2) + (aP)^2 + bP]$, where $P = (\max(F_o^2,\theta) + 2F_c^2)/3$.

spectrometer (^{1}H, 300 MHz; ^{13}C, 75.4 MHz) referenced to $SiMe_4$ or the solvent. CPMAS ^{13}C NMR spectra were recorded on a Brüker MSL 400P spectrometer at 100.6 MHz with a 4.5 μs 90° pulse, contact time of 2 ms. UV-Visible spectra were measured on a JASCO V-560 instrument. Microanalyses (C, H, N and S) were measured by the Department of Chemistry, University of Aveiro.

Acknowledgements

The authors would like to acknowledge Fundação para a Ciência e a Tecnologia (FCT) for financial support. S. M. O. Quintal thanks the FCT for a postgraduate grant. We also thank the EPSRC (UK) and the University of Reading (UK) for funds for the Image Plate System and Mr A. W. Johans for his assistance with the crystallography.

References

1 E. S. Raper, *Coord. Chem. Rev.*, 1996, **153**, 199.
2 E. S. Raper, *Coord. Chem. Rev.*, 1997, **165**, 475.
3 H. Engelking, S. Karentzopoulos, G. Reusmann and B. Krebs, *Chem. Ber.*, 1994, **127**, 2355.
4 A. J. Deeming, M. N. Meah, P. A. Bates and M. B. Hursthouse, *J. Chem. Soc., Dalton Trans.*, 1988, 2193.
5 Y. Nakatsu, Y. Nakamura, K. Matsumoto and S. Ooi, *Inorg. Chim. Acta*, 1992, **196**, 81.
6 J. L. Davidson, P. N. Preston and M. Russo, *J. Chem. Soc., Dalton Trans.*, 1983, 783.
7 J. H. Yanamoto, W. Yoshida and C. M. Jensen, *Inorg. Chem.*, 1991, **30**, 1353.
8 K. Umakoshi, I. Kinoshita and S. Ooi, *Inorg. Chim.Acta*, 1987, **127**, L41.
9 M. Gupta, R. E. Cramer, K. Ho, C. Pettersen, S. Mishina, J. Belli and C. M. Jensen, *Inorg. Chem.*, 1995, **34**, 60.
10 K. Umakoshi, I. Kinoshita, Y. F. Yasuba, K. Matsumoto, S. Ooi, H. Nakai and M. Shiro, *J. Chem. Soc., Dalton Trans.*, 1989, 815.
11 P. B. Kettler, Y. Chang, D. Rose, J. Zubieta and M. J. Abrams, *Inorg. Chim. Acta*, 1996, **244**, 199.
12 D. J. Rose, K. P. Maresca, T. Nicholson, A. Davison, A. G. Jones, J. Babich, A. Fishcman, W. Graham, J. R. D. DeFord and J. Zubieta, *Inorg. Chem.*, 1998, **37**, 2701.
13 K. Umakoshi, A. Ichimura, I. Kinoshita and S. Ooi, *Inorg. Chem.*, 1990, **29**, 4005.
14 K. Umakoshi, I. Kinoshita, A. Ichimura, K. Matsumoto and S. Ooi, *Inorg. Chem.*, 1987, **26**, 3551.
15 J. R. Dilworth, J. Hu, J. R. Miller, S. Lu and Q. Wu, *Polyhedron*, 1996, **15**, 953.
16 L. J. McCaffrey, W. Henderson, B. K. Nicholson, J. E. Mackay and M. B. Dinger, *J. Chem. Soc., Dalton Trans.*, 1997, 2577.
17 L. J. McCaffrey, W. Henderson and B. K. Nicholson, *Polyhedron*, 1998, **17**, 221.
18 W. Schneider, A. Bauer and H. Schmidbaur, *Organometallics*, 1996, **15**, 5445.
19 S. Mitra, H. Biswas and P. Bandyopadhyay, *Polyhedron*, 1997, **16**, 447.
20 F. N. Rein and H. E. Toma, *Polyhedron*, 1998, **17**, 1439.
21 E. W. Ainscough, A. M. Brodie, R. K. Coll, T. G. Kotch, A. J. Lees, A. J. A. Mair and J. M. Waters, *J. Organomet. Chem.*, 1996, **517**, 173.
22 L. Armijo and V. Arancibia, *Anal. Chim. Acta*, 1994, **298**, 91.
23 S. Marchal, V. Moreno, G. Aullón, S. Alvarez, M. Quirós, M. F. Bardia and X. Salans, *Polyhedron*, 1999, **18**, 3675.
24 K. Nomiya, S. Takahashi and R. Noguchi, *J. Chem. Soc., Dalton Trans.*, 2000, 2091.
25 K. Nomiya, R. Noguchi, T. Shigeta, Y. Kondoh, Kazuhiro Tsuda, K. Ohsawa, N. C. Kasuga and M. Oda, *Bull. Chem. Soc. Jpn.*, 2000, **73**, 1143.
26 P. J. Blower and J. R. Dilworth, *Coord. Chem. Rev.*, 1987, **76**, 121.
27 I. G. Dance, *Polyhedron*, 1986, **5**, 1037.
28 C. G. Kuehn and S. S. Isied, *Prog. Inorg. Chem.*, 1980, **27**, 153.
29 G. C. Tucci, J. P. Donahue and R. H. Holm, *Inorg. Chem.*, 1998, **37**, 1602.
30 C. Lorber, M. R. Plutino, L. I. Eldind and E. Nordlander, *J. Chem. Soc., Dalton Trans.*, 1997, 3997.
31 J. Berg and R. H. Holm, *J. Am. Chem. Soc.*, 1985, **107**, 925.
32 B. E. Schultz and R. H. Holm, *Inorg. Chem.*, 1993, **32**, 4244.
33 Y. Wong, J. Ma, W. Law, Y. Yan, W. Wong, Z. Zhang, T. C. W. Mak and D. K. P. Ng, *Eur. J. Inorg. Chem.*, 1999, 313.
34 H. Li, P. Palanca, V. Sanz and L. Lahoz, *Inorg. Chim. Acta*, 1999, **285**, 25.
35 S. N. Rao, K. N. Munshi, N. N. Rao, M. M. Bhadhade and E. Sureh, *Polyhedron*, 1999, **18**, 2491.
36 J. Berg and R. H. Holm, *J. Am. Chem. Soc.*, 1985, **107**, 917.
37 W. P. Griffith, H. I. S. Nogueira, B. C. Parkin, R. N. Sheppard, A. J. P. White and D. J. Williams, *J. Chem. Soc., Dalton Trans.*, 1995, 1775.
38 S. M. O. Quintal, H. I. S. Nogueira, V. Félix and M. G. B. Drew, *New J. Chem.*, 2000, **24**, 511.
39 S. M. O. Quintal, H. I. S. Nogueira, H. Carapuça, V. Félix and M. G. B. Drew, *J. Chem. Soc., Dalton Trans.*, 2001, 3196.
40 R. Battistuzi, T. Manfredi, L. P. Battaglia, A. B. Corradi and A. Marzotto, *J. Crystallogr. Spectrosc. Res.*, 1989, **19**, 513.
41 G. Battistuzi, M. Borsari and R. Battistuzi, *Polyhedron*, 1997, **16**, 2093.
42 G. Battistuzi, M. Cannio and R. Battistuzi, *Polyhedron*, 2000, **19**, 2163.
43 F. H. Allen, J. E. Davies, J. J. Galloy, O. Johnson, O. Kennard, C. F. Macrae and D. G. Watson, *J. Chem. Inf. Comput. Sci.*, 1991, **31**, 204.
44 H. I. S. Nogueira, *Spectrochim. Acta, Part A*, 1998, **54**, 1461.
45 D. K. Demertzi, P. Kyrkou and I. Zakharoba, *Polyhedron*, 1991, **10**, 1507.
46 P. A. P. Lourido, J. A. G. Vásquez, J. Romero, M. S. Louro, A. Sousa, Q. Chen, Y. Chang and J. Zubieta, *J. Chem. Soc., Dalton Trans.*, 1996, 2047.
47 S. Banerji, R. E. Byrne and S. E. Livingstone, *Transition Met. Chem.*, 1982, **7**, 5.

48 E. C. Constable, S. M. Elder, C. A. Palmer, P. R. Raithby and D. A. Tocher, *Inorg. Chim. Acta*, 1996, **252**, 281.
49 C. C. Landry, A. Hynes, A. R. Barron, I. Haiduc and C. Silvestru, *Polyhedron*, 1996, **15**, 391.
50 E. C. Constable, C. A. Palmer and D. A. Tocher, *Inorg. Chim. Acta*, 1990, **176**, 57.
51 M. D. Couce, G. Faraglia, U. Russo, L. Sindellari and G. Valle, *J. Organomet. Chem.*, 1996, **513**, 77.
52 C. F. Edwards, W. P. Griffith, A. J. P. White and D. J. Williams, *J. Chem. Soc., Dalton Trans.*, 1993, 3813.
53 C. J. Doonan, D. A. Slizys and C. G. Young, *J. Am. Chem. Soc.*, 1999, **121**, 6430.
54 M. Gielen, A. Khloufi, M. Biesemans, R. Willem and J. M. Piret, *Polyhedron*, 1992, **11**, 1861.
55 N. Ueyama, H. Oku, M. Kondo, T. Okamura, N. Yosjinaga and A. Nakamura, *Inorg. Chem.*, 1996, **35**, 643.
56 Y. Wong, Y. Yan, E. Chan, Q. Yang, T. C. W. Mak and D. K. P. Ng, *J. Chem. Soc., Dalton Trans.*, 1998, 3057.
57 L. Stelzig, S. Kötte and B. Krebs, *J. Chem. Soc., Dalton Trans.*, 1998, 2921.
58 J. A. Craig, E. W. Harlan, B. S. Snyder, M. A. Whitener and R. H. Holm, *Inorg. Chem.*, 1989, **28**, 2082.
59 R. C. Cookson and D. W. Jones, *J. Chem. Soc.*, 1965, 1881.
60 J. C. Bailar, Jr and H. Itatani, *Inorg. Chem.*, 1965, **4**, 1618.
61 W. P. Griffith and S. I. Mostafa, *Polyhedron*, 1992, **11**, 871.
62 G. F. Ciani, G. D'Alfonso, P. F. Romiti, A. Sironi and M. Freni, *Inorg. Chim. Acta*, 1983, **72**, 29.
63 G. J. J. Chen, J. W. McDonald and W. E. Newton, *Inorg. Chem.*, 1976, **15**, 2612.
64 W. Kabsch, *J. Appl. Crystallogr.*, 1988, **21**, 916.
65 DIFABS, N. Walker and D. Stuart, *Acta Crystallogr., Sect. A*, 1983, **39**, 158.
66 G. M. Sheldrick, SHELX-97, University of Göttingen, Germany, 1997.
67 A. L. Spek, PLATON, A Multipurpose Crystallographic Tool, Utrecht University, Utrecht, The Netherlands, 1999.